Available online at www.sciencedirect.com
ScienceDirect
International Journal of Thermal Sciences 47 (2008) 274–281
International Journal of Thermal Sciences
www.elsevier.com/locate/ijts

Thermoelastic response of a fin exhibiting elliptic thickness profile: An analytical solution

Ahmet N. Eraslan *, Turgut Tokdemir

Department of Engineering Sciences, Middle East Technical University, Ankara 06531, Turkey

Received 23 June 2006; received in revised form 11 January 2007; accepted 24 January 2007

Available online 27 March 2007

Abstract

A thermoelastic analytical solution of a variable thickness cooling fin problem is presented. A variable thickness annular fin mounted on a hot rotating rigid shaft is considered. The thickness of the fin is assumed to vary radially in a continuously variable nonlinear elliptic form. An energy equation that accounts for the conduction, convective heat loss from peripheral and edge surfaces, thickness variation and rotation is adopted. The thermoelastic equation is obtained under formal assumptions of plane stress and small strains. For given heat and centrifugal loads the temperature distribution in the fin and the corresponding state of stress are obtained by means of the analytical solutions of energy and thermoelastic equations, respectively.

Keywords: Thermoelasticity; Cooling fin; Variable thickness; Stress analysis; Rotation; Thermal effects

1. Introduction

In a recent investigation by Eraslan and Akis [1], a realistic conduction–convection mechanism to describe the heat flow in uniform thickness annular fins was proposed. This mechanism was used in [1] to predict the elastoplastic stress state in a fin mounted on a rigid rotating shaft. An extension of this work was later realized by Eraslan and Kartal [2] to include a fin of parabolic thickness with temperature dependent material properties. The latter theoretical investigation was computational; however, some analytical results based on earlier solutions [3] were also presented.

This work represents an extension of [1] to include a variable thickness fin and presents an exclusive analytical treatment of a similar problem in the elastic state of stress. A variable thickness annular fin mounted on a rigid shaft is considered. The geometry of the shaft-fin assembly and the coordinate system are depicted in Fig. 1. The shaft is assumed to be kept at constant temperature. Heat is transferred from hot shaft to annular fin and from fin to surroundings. Moreover, the assembly may rotate about the axis of the shaft. The fin thickness h varies in the radial direction r according to

$$h(r) = h_0\sqrt{1 - n\left(\frac{r}{b}\right)^2} \tag{1}$$

in which n is a geometric parameter ($0 \leqslant n < 1$), b is the radius of the fin and h_0 is the thickness at the axis of the fin. The elliptic annular fin of inner radius $a/b = 0.2$ for $n = 0.7$ is shown in Fig. 2. The objective is to predict the elastic response of the elliptic fin under nonuniform heating or both heating and centrifugation.

Estimation of the stresses, vibrations and heat transfer in disks/fins induced by centrifugation or nonuniform heating or both is an important topic due to a large number of applications in many branches of engineering [4–10]. Therefore, the interest of researchers in the subject has never ceased. However, there appear only a few investigations in the literature on the deformations and heat transfer in disks/fins subjected to both centrifugal force and radial temperature gradients. In addition to the ones mentioned above [1,2], theoretical studies by Alujevic et al. [11,12], by Parmaksızoğlu and Güven [13], and experimental work by Saniei and Yan [14] may be quoted as closely related references.

* Corresponding author.
E-mail address: aeraslan@metu.edu.tr (A.N. Eraslan).

1290-0729/$ – see front matter
doi:10.1016/j.ijthermalsci.2007.01.030

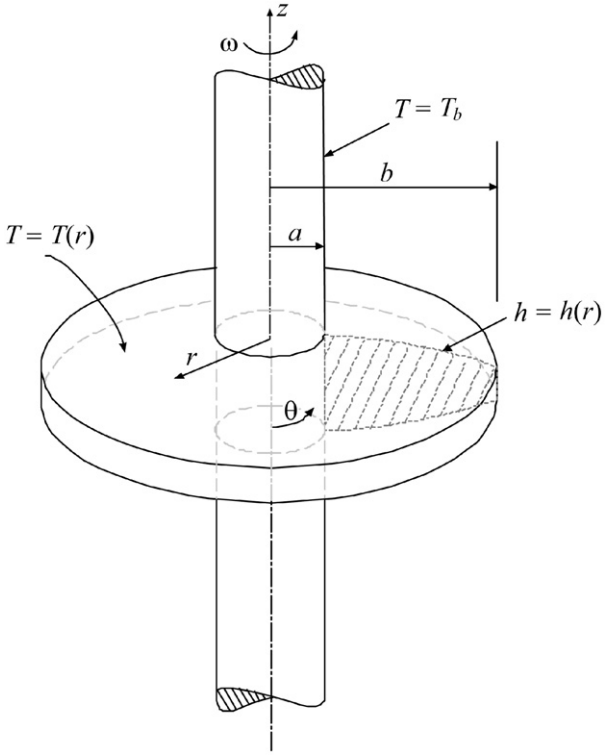

Fig. 1. The geometry of the shaft-fin assembly and the coordinate system.

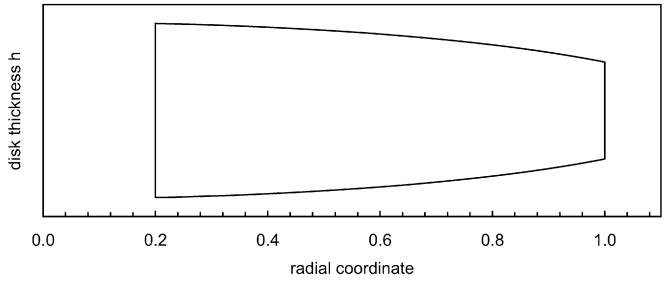

Fig. 2. Elliptic thickness profile for a fin of inner radius $a/b = 0.2$ for $n = 0.7$.

2. Temperature distribution in the fin

For constant thermal conductivity k of the fin material, the energy equation given in Ref. [2] takes the form

$$\frac{\mathrm{d}^2\Theta}{\mathrm{d}r^2} + \left[\frac{1}{r} + \frac{h'(r)}{h(r)}\right]\frac{\mathrm{d}\Theta}{\mathrm{d}r} - \frac{2H_c}{kh(r)}\Theta = 0 \tag{2}$$

where $\Theta(r) = T(r) - T_0$ is the temperature difference between the surface of the fin and the ambient temperature, H_c is the convective heat transfer coefficient, and a prime denotes differentiation with respect to the radial coordinate r. H_c is a function of both the radial position r and angular speed ω, given by $H_c(r,\omega) = A + B\omega r$ with A and B being parameters. Substituting the thickness function h from Eq. (1) and H_c into Eq. (2), the energy equation becomes

$$\frac{\mathrm{d}^2\Theta}{\mathrm{d}r^2} + \left[\frac{1}{r} - \frac{nr}{b^2(1-\frac{nr^2}{b^2})}\right]\frac{\mathrm{d}\Theta}{\mathrm{d}r} - \frac{2(A+B\omega r)}{kh_0\sqrt{1-\frac{nr^2}{b^2}}}\Theta = 0 \tag{3}$$

The general solution of this differential equation is obtained by reduction of order as

$$\Theta(r) = C_1 P(r) + C_2 Q(r) \tag{4}$$

where C_i is an arbitrary constant and

$$P(r) = \sum_{k=0}^{\infty} a_k r^k \tag{5}$$

The first few coefficients are

$$a_0 = 1 \tag{6}$$

$$a_1 = 0 \tag{7}$$

$$a_2 = \frac{A}{2kh_0} \tag{8}$$

$$a_3 = \frac{2B\omega}{9kh_0} \tag{9}$$

$$a_4 = \frac{A(Ab^2 + 2knh_0)}{16b^2k^2h_0^2} \tag{10}$$

$$a_5 = \frac{B\omega(13Ab^2 + 15knh_0)}{225b^2k^2h_0^2} \tag{11}$$

$$a_6 = \frac{9A(A^2b^4 + 8Ab^2knh_0 + 18k^2n^2h_0^2) + 32b^4B^2kh_0\omega^2}{2592b^4k^3h_0^3} \tag{12}$$

$$a_7 = \frac{B\omega(433A^2b^4 + 2510Ab^2knh_0 + 3150k^2n^2h_0^2)}{88\,200b^4k^3h_0^3} \tag{13}$$

$$a_8 = \big[225A\big(A^3b^6 + 20A^2b^4knh_0 + 150Ab^2k^2n^2h_0^2 + 360k^3n^3h_0^3\big) + 32b^4B^2kh_0\omega^2\big(142Ab^2 + 435knh_0\big)\big] \big/ \big(2\,073\,600b^6k^4h_0^4\big) \tag{14}$$

and

$$Q(r) = P(r)\left[\frac{\ln r}{b} + \sum_{k=0}^{\infty} d_k r^k\right] \tag{15}$$

with the following coefficients

$$d_0 = 0 \tag{16}$$

$$d_1 = 0 \tag{17}$$

$$d_2 = \frac{n - 4b^2a_2}{4b^3} \tag{18}$$

$$d_3 = -\frac{2a_3}{3b} \tag{19}$$

$$d_4 = \frac{3n^2 - 8b^2na_2 + 24b^4a_2^2 - 16b^4a_4}{32b^5} \tag{20}$$

$$d_5 = -\frac{na_3 - 6b^2a_2a_3 + 2b^2a_5}{5b^3} \tag{21}$$

$$d_6 = \big[5n^3 - 12b^2n^2a_2 + 24b^4na_2^2 - 64b^6a_2^3 + 48b^6a_3^2 - 16b^4na_4 + 96b^6a_2a_4 - 32b^6a_6\big]\big/\big(96b^7\big) \tag{22}$$

$$d_7 = -\big(3n^2a_3 - 12b^2na_2a_3 + 48b^4a_2^2a_3 - 24b^4a_3a_4 + 4b^2na_5 - 24b^4a_2a_5 + 8b^4a_7\big)\big/\big(28b^5\big) \tag{23}$$

$$d_8 = \big[35n^4 - 80b^2n^3a_2 + 144b^4n^2a_2^2 - 256b^6na_2^3 + 640b^8a_2^4 + 192b^6na_3^2 - 1536b^8a_2a_3^2 - 96b^4n^2a_4 + 384b^6na_2a_4 - 1536b^8a_2^2a_4 + 384b^8a_4^2 + 768b^8a_3a_5 - 128b^6na_6 + 768b^8a_2a_6 - 256b^8a_8\big]/\big(1024b^9\big) \quad (24)$$

It is noted that these coefficients and higher order ones can be generated by the use of symbolic engine Maple with the series option turned on [15]. In view of Eq. (4), the temperature distribution in the fin is

$$T(r) = C_1P(r) + C_2Q(r) + T_0 \quad (25)$$

Integration constants C_1 and C_2 are determined by using the following boundary conditions (see Fig. 1):

$$T(a) = T_b \quad \text{and} \quad -k\frac{\mathrm{d}T}{\mathrm{d}r}\bigg|_{r=b} = H_c(b,\omega)\big[T(b) - T_0\big] \quad (26)$$

The result is

$$C_1 = -(T_b - T_0)\big[H_c(b,\omega)Q(b) + kQ'(b)\big] \big/\big(H_c(b,\omega)P(b)Q(a) + kQ(a)P'(b) - P(a)\big[H_c(b,\omega)Q(b) + kQ'(b)\big]\big) \quad (27)$$

$$C_2 = (T_b - T_0)\big[H_c(b,\omega)P(b) + kP'(b)\big] \big/\big(H_c(b,\omega)P(b)Q(a) + kQ(a)P'(b) - P(a)\big[H_c(b,\omega)Q(b) + kQ'(b)\big]\big) \quad (28)$$

For the presentation of calculated temperature distributions, it is convenient to introduce the following dimensionless variables:

$$\text{Radial coordinate:} \quad \bar{r} = \frac{r}{b} \quad (29)$$

$$\text{Temperature:} \quad \theta = \frac{T - T_0}{T_b - T_0} \quad (30)$$

$$\text{Temperature gradient:} \quad G_T = \frac{\mathrm{d}T/\mathrm{d}r}{\mathrm{d}T/\mathrm{d}r|_{\{r=a,\ \omega=0\}}} \quad (31)$$

$$\text{Angular speed:} \quad \Omega = b\omega\sqrt{\frac{\rho}{\sigma_0}} \quad (32)$$

$$\text{Heat load:} \quad \bar{q} = \frac{E\alpha T_b}{\sigma_0 \log(\frac{b}{a})} \quad (33)$$

$$\text{Heat transfer coefficient:} \quad \overline{H_c} = 1 + \overline{B}\Omega\bar{r};\ \overline{B} = \frac{B}{A}\sqrt{\frac{\sigma_0}{\rho}} \quad (34)$$

where E is the modulus of elasticity, α the coefficient of thermal expansion, σ_0 the yield limit and ρ the mass density.

First, the convergence of the series solution, Eq. (25), is inspected. Preliminary calculations indicate that the solution converges very rapidly for a wide range of parameters; nevertheless, it is affected mostly by the values of the parameters n and Ω. Using the parameters $\bar{a} = a/b = 0.2$, $\bar{h}_0 = h_0/b = 0.2$ (thin fin), $\overline{B} = 1.5$ and assigning $\bar{q} = 1$, the temperatures at the edge of the fin, $\theta(1)$, are calculated with an increasing number of terms in the series and the corresponding relative percent errors are calculated by the use of $|\theta(1) - \theta_T(1)|/\theta_T(1) \times 100$. Here, $\theta_T(1)$ represents the solution with 35 terms. The results of these calculations are presented in Fig. 3(a) for $n = 0.4$, and in Fig. 3(b) for $n = 0.6$ using Ω as a parameter. As seen in these figures, a reasonably accurate solution may be obtained by including the first 20 terms (Fig. 3(b)) though 35 terms are used throughout this work to assure accuracy.

The analytical results for $\theta_T(1)$ are also compared with numerical results based on the Shooting solution of Eq. (3). As explained in Refs. [1,2], when incorporated with the state-of-the-art ODE solvers [16] such solutions produce results possessing very high order accuracy. For the same set of parameters and for $n = 0.6$, $\theta_T(1)$ values corresponding to $\Omega = 0$, 1, and 2 are 0.592760, 0.382905, and 0.273655, respectively. On the other hand, the matching shooting results are $\theta(1) = 0.592750$, 0.382894, and 0.273644. Both solutions agree well.

To give an idea about the magnitudes of some variables of engineering interest, we list several numerical values. Material properties of steel: $k = 45$ W/m °C, $E = 200$ GPa, $\alpha = 11.7 \times 10^{-6}$/°C, $\sigma_0 = 410$ MPa, and $\rho = 7800$ kg/m^3 are used for this purpose. The parameter set $\bar{a} = 0.2$, $n = 0.6$, $\bar{h}_0 = 0.2$, and $\overline{B} = 1.5$ is reconsidered, and $T_0 = 0$ is assigned. The heat load $\bar{q} = 1$ gives rise to temperatures $T(a) = 122.5$ °C, and $T(b) = 72.6$ °C for $\Omega = 0$, and $T(a) = 122.5$ °C, and $T(b) = 33.5$ °C for $\Omega = 2$. Furthermore, for steel fins the speeds $\Omega = 1$, and 2 imply 229.3 rad/s and 458.5 rad/s, actual rotation speeds, respectively.

Using the parameters $\bar{a} = 0.2$, $n = 0.6$, $\bar{h}_0 = 0.2$, and $\overline{B} = 1.5$, and setting $\bar{q} = 1$, temperature distributions and corresponding temperature gradients are calculated at various angular velocities ranging from $\Omega = 0$ to $\Omega = 1.5$ and the results are plotted in Figs. 4(a) and (b). Fig. 4(a) shows the temperature profiles using the angular speed as a parameter. Due to the increasing rate of convective heat transfer, the lowest temperature at the edge of the disk is obtained for the largest angular speed. Fig. 4(b) shows the radial variation of temperature gradient G_T at various rotation speeds. Larger gradients are obtained as the angular speed is increased.

3. Thermoelastic formulation and solution

The notation and basic equations of elasticity as given by Timoshenko and Goodier [5] are used. A state of plane stress and infinitesimal deformations are assumed. For plane stress, the solution of the displacement-stress relations

$$\frac{u}{r} = \frac{1}{E}(\sigma_\theta - \nu\sigma_r) + \alpha T \quad (35)$$

$$\frac{\mathrm{d}u}{\mathrm{d}r} = \frac{1}{E}(\sigma_r - \nu\sigma_\theta) + \alpha T \quad (36)$$

for σ_r and σ_θ gives

$$\sigma_r = \frac{E}{1-\nu^2}\left[\frac{\nu u}{r} + u'\right] - \frac{E\alpha T}{1-\nu} \quad (37)$$

$$\sigma_\theta = \frac{E}{1-\nu^2}\left[\frac{u}{r} + \nu u'\right] - \frac{E\alpha T}{1-\nu} \quad (38)$$

where u is the radial displacement, σ_j the normal stress, ν the Poisson's ratio and T the temperature gradient. Substitution of these stresses and the fin profile (1), in the equation of motion [5]

$$\frac{\mathrm{d}}{\mathrm{d}r}(hr\sigma_r) - h\sigma_\theta = -h\rho\omega^2r^2 \quad (39)$$

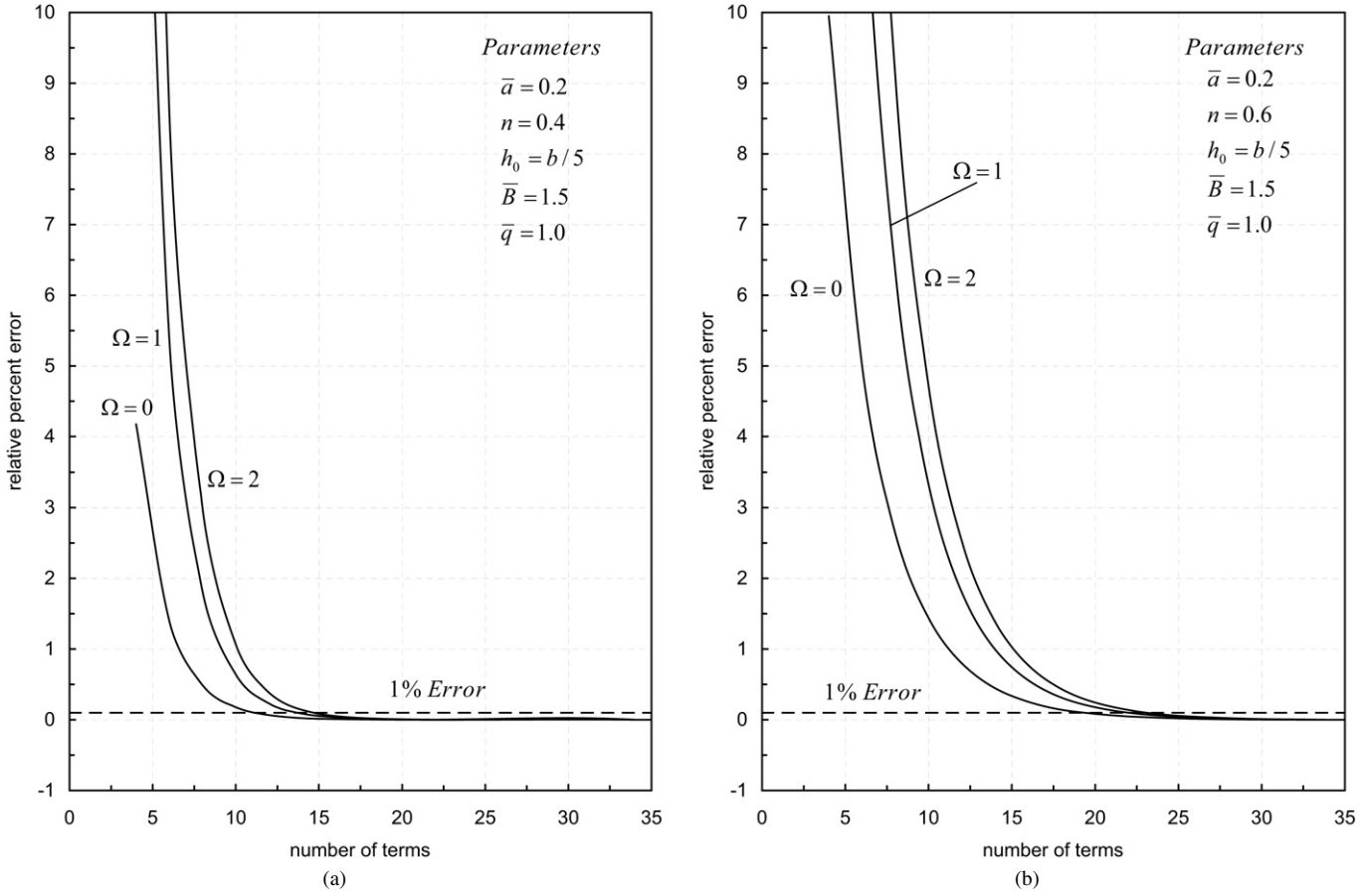

Fig. 3. Variation of relative percent error in the edge temperature with the number of terms (a) for $n = 0.4$, (b) for $n = 0.6$.

yields the governing equation for the radial displacement.

$$r^2\left(b^2 - nr^2\right)\frac{\mathrm{d}^2u}{\mathrm{d}r^2} + r\left(b^2 - 2nr^2\right)\frac{\mathrm{d}u}{\mathrm{d}r} - \left[b^2 - (1-\nu)nr^2\right]u = -\frac{(b^2 - nr^2)(1-\nu^2)\rho\omega^2 r^3}{E} - n\alpha(1+\nu)r^3T + \alpha\left(b^2 - nr^2\right)(1+\nu)r^2\frac{\mathrm{d}T}{\mathrm{d}r} \tag{40}$$

Eq. (40) is a hypergeometric differential equation and can be solved by introducing a new variable $z = b^2 - nr^2$ and using the transformation $u(r) = ry(z)$. The homogeneous equation is transformed into

$$z\left(b^2 - z\right)\frac{\mathrm{d}^2y}{\mathrm{d}z^2} + \frac{1}{2}\left(b^2 - 5z\right)\frac{\mathrm{d}y}{\mathrm{d}z} - \frac{(1+\nu)}{4}y = 0 \tag{41}$$

This is the standard form of the hypergeometric differential equation with the solution [17]

$$y(z) = C_3F\left(\alpha, \beta, \delta; \frac{z}{b^2}\right) + C_4\sqrt{z}F\left(\alpha - \delta + 1, \beta - \delta + 1, 2 - \delta; \frac{z}{b^2}\right) \tag{42}$$

where $F(\alpha, \beta, \delta; z)$ is the hypergeometric function defined by

$$F(\alpha, \beta, \delta; z) = 1 + \frac{\alpha\beta}{\delta 1!}z + \frac{\alpha(\alpha+1)\beta(\beta+1)}{\delta(\delta+1)2!}z^2 + \frac{\alpha(\alpha+1)(\alpha+2)\beta(\beta+1)(\beta+2)}{\delta(\delta+1)(\delta+2)3!}z^3 + \cdots \tag{43}$$

The series $F(\alpha, \beta, \delta; z)$ converges slowly for $|z| \leqslant 1$ provided that $\delta - (\alpha + \beta) > -1$. Since the problem under consideration is a realistic physical problem, these conditions are always satisfied and the series is always convergent. The arguments α, β and δ of the hypergeometric function F in Eq. (42) have the following meanings:

$$\alpha = \frac{3}{4} - \frac{1}{4}\sqrt{5 - 4\nu} \tag{44}$$

$$\beta = \frac{3}{4} + \frac{1}{4}\sqrt{5 - 4\nu} \tag{45}$$

$$\delta = \frac{1}{2} \tag{46}$$

The general solution for the radial displacement can thus be expressed as

$$u(r) = C_3P(r) + C_4Q(r) + R(r) \tag{47}$$

where

$$P(r) = rF\left(\alpha, \beta, \delta; 1 - n\left(\frac{r}{b}\right)^2\right) \tag{48}$$

$$Q(r) = r\sqrt{b^2 - nr^2} \times F\left(\alpha - \delta + 1, \beta - \delta + 1, 2 - \delta; 1 - n\left(\frac{r}{b}\right)^2\right) \tag{49}$$

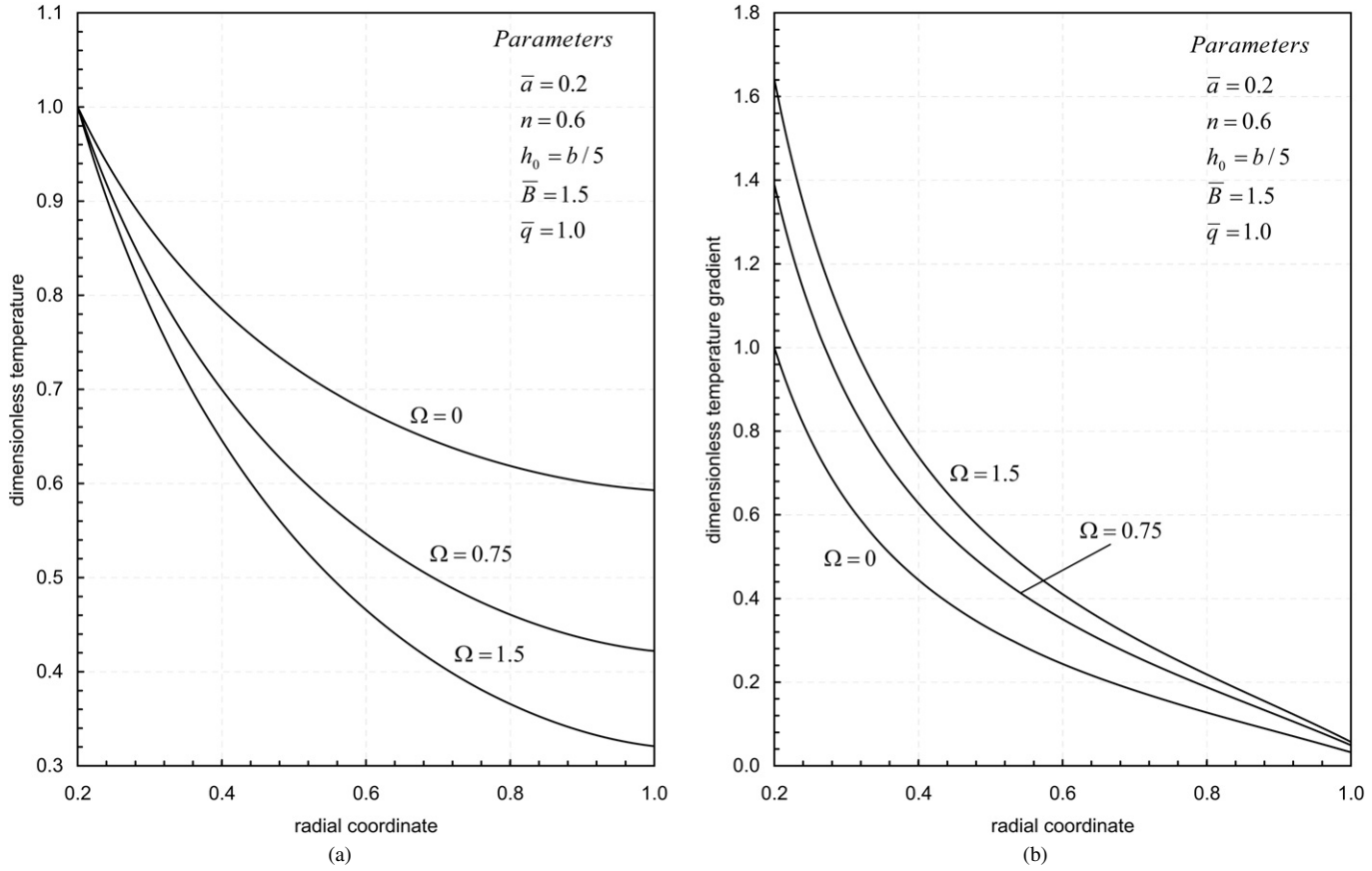

Fig. 4. (a) Temperature profiles, (b) temperature gradient profiles at various rotation speeds.

and $R(r)$ represents the particular integral solution. R is determined by the method of variation of parameters. It is assumed to be of the form

$$R(r) = \widehat{U}_1(r)P(r) + \widehat{U}_2(r)Q(r) \tag{50}$$

where

$$\widehat{U}_1(r) = -\int_a^r G_1(\lambda)\,\mathrm{d}\lambda; \qquad \widehat{U}_2(r) = \int_a^r G_2(\lambda)\,\mathrm{d}\lambda \tag{51}$$

$$G_1(r) = \frac{Q(r)f(r)}{W_{ro}(r)}; \qquad G_2(r) = \frac{P(r)f(r)}{W_{ro}(r)} \tag{52}$$

$$f(r) = -\frac{(1-\nu^2)\rho\omega^2 r}{E} - \frac{n\alpha(1+\nu)rT}{b^2-nr^2} + \alpha(1+\nu)\frac{\mathrm{d}T}{\mathrm{d}r} \tag{53}$$

$$W_{ro}(r) = P(r)Q'(r) - Q(r)P'(r) \tag{54}$$

Since the integrands in Eq. (51) are polynomials, the integrals can accurately be evaluated by expanding them into series at Gaussian points [7]. Hence, $\widehat{U}_1$ and $\widehat{U}_2$ take the following forms

$$\widehat{U}_1(r) = \frac{r-a}{2}\sum_{i=1}^{N}\phi_i \times G_1\left(\frac{(r-a)X_i + r + a}{2}\right) \tag{55}$$

$$\widehat{U}_2(r) = \frac{r-a}{2}\sum_{i=1}^{N}\phi_i \times G_2\left(\frac{(r-a)X_i + r + a}{2}\right) \tag{56}$$

where the values of ϕ_i and X_i can be found in [18] for possible values of N used in practice. In the following calculations $N = 20$. With the form (47) of the radial displacement, the stresses become

$$\sigma_r = \frac{E}{1-\nu^2}\left[C_3\left(\frac{\nu P}{r} + P'\right) + C_4\left(\frac{\nu Q}{r} + Q'\right) + \frac{\nu R}{r} + R'\right] - \frac{E\alpha T}{1-\nu} \tag{57}$$

$$\sigma_\theta = \frac{E}{1-\nu^2}\left[C_3\left(\frac{P}{r} + \nu P'\right) + C_4\left(\frac{Q}{r} + \nu Q'\right) + \frac{R}{r} + \nu R'\right] - \frac{E\alpha T}{1-\nu} \tag{58}$$

The thermoelastic solution is completed by applying the boundary conditions. Since an elliptic annular fin mounted on a rigid shaft is considered, the boundary conditions become $u(a) = 0$ and $\sigma_r(b) = 0$. By noting that $R(a) = 0$, the integration constants are evaluated as

$$C_3 = -\frac{Q(a)[\nu R(b) + bR'(b) - b\alpha(1+\nu)T(b)]}{Q(a)[\nu P(b) + bP'(b)] - P(a)[\nu Q(b) + bQ'(b)]} \tag{59}$$

$$C_4 = \frac{P(a)[\nu R(b) + bR'(b) - b\alpha(1+\nu)T(b)]}{Q(a)[\nu P(b) + bP'(b)] - P(a)[\nu Q(b) + bQ'(b)]} \tag{60}$$

Note also that for $n = 0$ and $T(r) = T_b = T_0$, Eq. (40) reduces to

$$r^2\frac{\mathrm{d}^2u}{\mathrm{d}r^2} + r\frac{\mathrm{d}u}{\mathrm{d}r} - u = -\frac{(1-\nu^2)\rho\omega^2 r^3}{E} \tag{61}$$

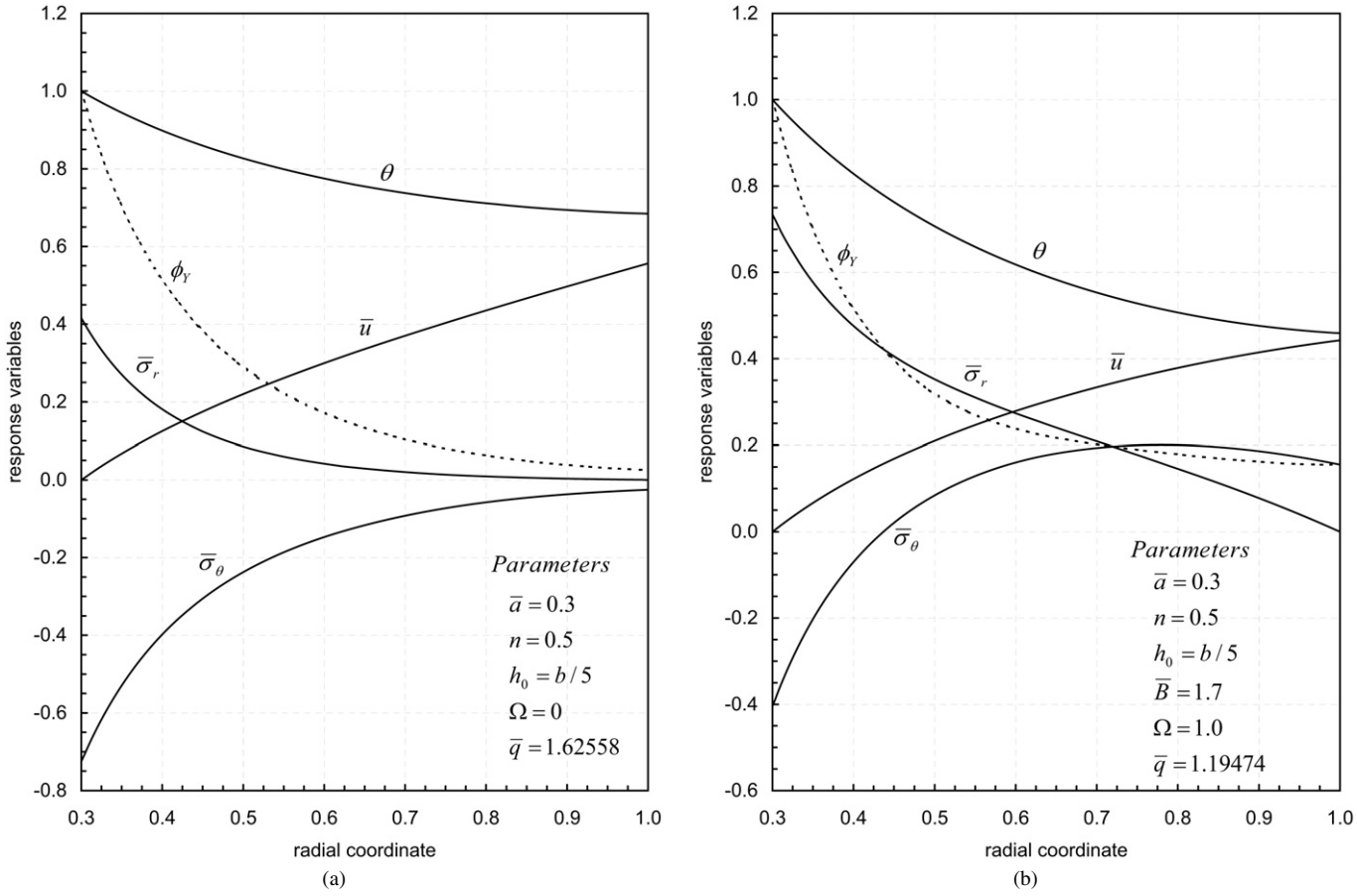

Fig. 5. Elastic response of (a) a stationary fin, (b) a rotating fin.

and assumes the general solution

$$u(r) = \widehat{C}_3 r + \frac{\widehat{C}_4}{r} - \frac{(1-\nu^2)\rho\omega^2 r^3}{8E} \tag{62}$$

which is the well-known solution of rotating isothermal uniform thickness disk [5].

To present the results of thermoelastic calculations we use nondimensional stress: $\overline{\sigma}_j = \sigma_j/\sigma_0$, and radial displacement: $\overline{u} = uE/(b\sigma_0)$. Moreover, we introduce the nondimensional stress variable ϕ_Y as

$$\phi_Y = \sqrt{\overline{\sigma}_r^2 - \overline{\sigma}_r\overline{\sigma}_\theta + \overline{\sigma}_\theta^2} \tag{63}$$

Note that according to the von Mises' yield criterion [19], $\phi_Y(r_Y) = 1$ at an elastic-plastic border implying the onset of plasticization at that radial location, and $\phi_Y < 1$ in the elastic region. In the following calculations $\nu = 0.3$.

For a stationary thin fin ($\Omega = 0$, $\bar{h}_0 = 0.2$) of inner radius $\overline{a} = 0.3$ with the shape parameter $n = 0.5$, the elastic limit heat load is determined as $\bar{q} = 1.62558$. Fig. 5(a) depicts the corresponding distributions of the response variables: $\overline{\sigma}_r$, $\overline{\sigma}_\theta$, $\overline{u}$, ϕ_Y, and θ. Since expansion at the rigid shaft-annular fin interface is not allowed, the circumferential stress turns out to be compressive. By following the variation of ϕ_Y, it is seen in Fig. 5(a) that the fin material fails with respect to plastic deformation at the shaft-fin interface since $\phi_Y = 1$ at this radial position. If the speed of rotation is slowly increased from $\Omega = 0$ to $\Omega = 1$, the fin yields at a much lower heat load calculated as $\bar{q} = 1.19474$. The consequent distributions of the response variables are plotted in Fig. 5(b). The superposition of thermal and centrifugal effects can be observed by comparing Figs. 5(a) and (b). This superposition, as well as the effect of n on the calculated elastic limits, can be evaluated by examining the results of a parametric analysis shown in Fig. 6. In this figure, using $\overline{a} = 0.3$ and $\overline{B} = 1.6$, elastic limit rotation speeds leading to $\phi_Y(a) = 1$ are calculated for different values of the shape parameter n using the heat load $\bar{q}$ as a parameter. As seen in Fig. 6, for a given Ω, the fin can withstand higher heat loads elastically if n is increased.

The approach described by Eqs. (55)–(56) to determine the particular solution, Eq. (50), was suggested by Uğural and Fenster [7] and used successfully in studies [3,20–22] in order to derive consistent analytical solutions to highly intricate rotating partially plastic solid disk problems. However, a discussion on this issue could not be found in the related literature. To comment on it, an analysis is carried out here. The parameter set $\overline{a} = 0.3$, $n = 0.5$, and $\overline{B} = 1.7$ is chosen. The elastic limit heat loads for $\Omega = 0$, and $\Omega = 1$ are calculated by using $N = 20$ and the results are cross checked with those of the Shooting solution of Eq. (40). By using a different number of Gaussian points, the elastic limit is determined and the corresponding relative percent error is calculated. The results of these calculations can be

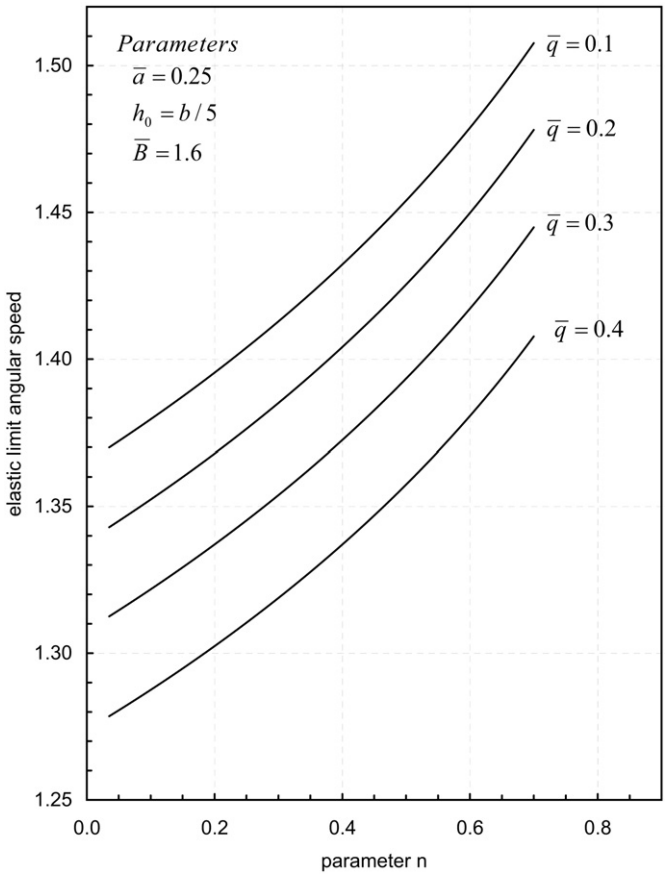

Fig. 6. Variation of elastic limit angular speeds with n for different heat loads.

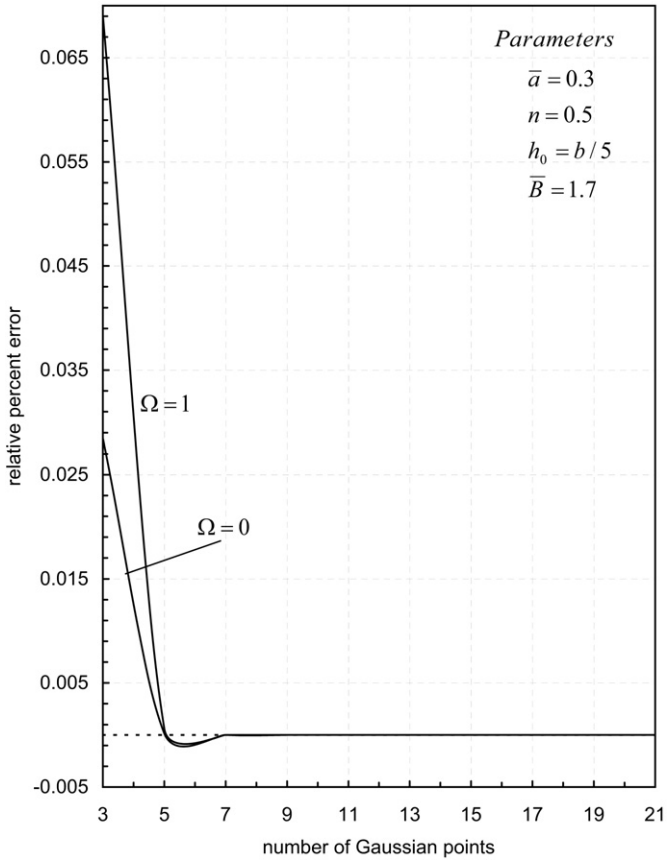

Fig. 7. Variation of relative percent error in the elastic limit heat load with the number of Gaussian points.

examined in Fig. 7. As seen in this figure, a reasonably accurate solution seems to be possible even with $N = 3$.

4. Concluding remarks

Based on the assumptions of plane stress, infinitesimal deformations, and low rotation frequencies, a thermoelastic analytical solution of a variable thickness cooling fin has been presented. An elliptic annular fin mounted on a hot rigid shaft, which may rotate about its axis, has been considered. A series solution to the energy equation that accounts for the conduction, convection, thickness variation and rotation has been obtained and its rate of convergence has been assessed. Displacement formulation has been used to construct the thermoelastic equation. This equation turns out to be of hypergeometric-type, and its homogeneous solution has been obtained in terms of hypergeometric functions by the introduction of an elliptic transformation. The method of variation of parameters has been combined with Gaussian integration to obtain the particular solution. Since the integrands involved are polynomials, this procedure does not affect the accuracy of the solution in any way.

The effect of rotation on the thermal and mechanical responses of the fin has been investigated. Larger temperature gradients are obtained as the rotation frequency is increased. Under purely thermal loading of the fin, the circumferential stress component is compressive in the majority of the fin. A transition from compressive to tensile stress states occurs as the thermally loaded fin is rotated. The fin can withstand higher heat loads or rotation speeds elastically if its inner-to-outer thickness ratio, i.e. $h(a)/h(b)$, is increased.

Acknowledgements

The authors take this opportunity to thank Ms. Yeşim Çöteli and Mr. Robert West in the School of Foreign Languages at METU for carefully editing the manuscript.

References

[1] A.N. Eraslan, T. Akis, On the elastic–plastic deformation of a rotating disk subjected to a radial temperature gradient, Mechanics Based Design of Structures and Machines 31 (4) (2003) 529–561.
[2] A.N. Eraslan, M.E. Kartal, Stress distributions in cooling fins of variable thickness with and without rotation, Journal of Thermal Stresses 28 (8) (2005) 861–883.
[3] A.N. Eraslan, Elastoplastic deformations of rotating parabolic solid disks using Tresca's yield criterion, European Journal of Mechanics A/Solids 22 (6) (2003) 861–874.
[4] B.A. Boley, J.H. Weiner, Theory of Thermal Stresses, Wiley, New York, 1960.
[5] S. Timoshenko, J.N. Goodier, Theory of Elasticity, third ed., McGraw-Hill, New York, 1970.
[6] D.W.A. Rees, The Mechanics of Solids and Structures, McGraw-Hill, New York, 1990.
[7] A.C. Uğural, S.K. Fenster, Advanced Strength and Applied Elasticity, third ed., Prentice-Hall International, London, 1995.

[8] C.D. Mote, Theory of thermal natural frequency variations in disks, International Journal of Mechanical Sciences 8 (8) (1966) 547–557.
[9] A.C.J. Luo, C.D. Mote, Nonlinear vibration of rotating thin disks, Journal of Vibration and Acoustics—Trans. ASME 122 (4) (2000) 376–383.
[10] N. Saniei, A.C.J. Luo, Thermally induced, nonlinear vibrations of rotating disks, Nonlinear Dynamics 26 (4) (2001) 393–409.
[11] A. Alujevic, J. Legat, J. Zupec, Thermal yield of a rotating hyperbolic disk, The Journal of Applied Mathematics and Mechanics (ZAMM) 73 (1993) T283–T287.
[12] A. Alujevic, P. Les, J. Zupec, Plasticity of a thermally loaded rotating hyperbolic disk, The Journal of Applied Mathematics and Mechanics (ZAMM) 73 (1993) T287–T290.
[13] C. Parmaksızoğlu, U. Güven, Plastic stress distribution in a rotating disk with rigid inclusion under a radial temperature gradient, Mechanics of Structures and Machines 26 (1998) 9–20.
[14] N. Saniei, X.J. Yan, An experimental study of heat transfer from a disk rotating in an infinite environment including heat transfer enhancement by jet impingement cooling, Journal of Enhanced Heat Transfer 7 (4) (2000) 231–245.
[15] F. Garvan, The Mapple Book, CRC Press, New York, 2002.
[16] N.P. Brown, A.C. Hindmarsh, Reduced storage matrix methods in stiff ODE systems, Applied Mathematics and Computation 31 (1) (1989) 40–91.
[17] S. Zhang, J. Jin, Computation of Special Functions, John Wiley & Sons, New York, 1996.
[18] M. Abromowich, I.A. Stegun (Eds.), Handbook of Mathematical Functions, fifth printing, U.S. Government Printing Office, Washington, DC, 1964.
[19] A.N. Eraslan, Von mises yield criterion and nonlinearly hardening variable thickness rotating annular disks with rigid inclusion, Mechanics Research Communications 29 (5) (2002) 339–350.
[20] A.N. Eraslan, Y. Orcan, Elastic–plastic deformation of a rotating solid disk of exponentially varying thickness, Mechanics of Materials 34 (7) (2002) 423–432.
[21] Y. Orcan, A.N. Eraslan, Elastic–plastic stresses in linearly hardening rotating solid disks of variable thickness, Mechanics Research Communications 29 (4) (2002) 269–281.
[22] A.N. Eraslan, Y. Orcan, On the rotating elastic–plastic solid disks of variable thickness having concave profiles, International Journal of Mechanical Sciences 44 (7) (2002) 1445–1466.